Available online at www.sciencedirect.com
SCIENCE DIRECT®
Journal of Solid State Chemistry 178 (2005) 3233–3242
JOURNAL OF SOLID STATE CHEMISTRY
www.elsevier.com/locate/jssc

REAuAl$_4$Ge$_2$ and REAuAl$_4$(Au$_x$Ge$_{1-x}$)$_2$ (RE = rare earth element): Quaternary intermetallics grown in liquid aluminum

Xiuni Wu, Mercouri G. Kanatzidis*

Department of Chemistry, Michigan State University, East Lansing, Michigan 48824, USA

Received 11 May 2005; received in revised form 22 July 2005; accepted 26 July 2005
Available online 8 September 2005

Abstract

The two families of intermetallic phases REAuAl$_4$Ge$_2$ (1) (RE = Ce, Pr, Nd, Sm, Eu, Gd, Tb, Dy, Er, Tm and Yb) and REAuAl$_4$(Au$_x$Ge$_{1-x}$)$_2$ (2) ($x = 0.4$) (RE = Ce and Eu) were obtained by the reactive combination of RE, Au and Ge in liquid aluminum. The structure of (1) adopts the space group R-3m (CeAuAl$_4$Ge$_2$, $a = 4.2384(7)$ Å, $c = 31.613(7)$ Å; NdAuAl$_4$Ge$_2$, $a = 4.2258(4)$ Å, $c = 31.359(5)$ Å; GdAuAl$_4$Ge$_2$, $a = 4.2123(6)$ Å, $c = 30.994(6)$ Å; ErAuAl$_4$Ge$_2$, $a = 4.2074(4)$ Å, $c = 30.717(5)$ Å). The structure of (2) adopts the tetragonal space group $P4/mmm$ with lattice parameters: $a = 4.3134(8)$ Å, $c = 8.371(3)$ Å for EuAuAl$_4$(Au$_x$Ge$_{1-x}$)$_2$ ($x = 0.4$). Both structure types present slabs of "AuAl$_4$Ge$_2$" or "AuAl$_4$(Au$_x$Ge$_{1-x}$)$_2$" stacking along the c-axis with layers of RE atoms in between. Magnetic susceptibility measurements indicate that the RE atoms (except for Ce and Eu) possess magnetic moments consistent with +3 species. The Ce atoms in CeAuAl$_4$Ge$_2$ and CeAuAl$_4$(Au$_x$Ge$_{1-x}$)$_2$ ($x = 0.4$) appear to be in a mixed +3/+4 valence state; DyAuAl$_4$Ge$_2$ undergoes an antiferromagnetic transition at 11 K and below this temperature exhibits metamagnetic behavior. The Eu atoms in EuAuAl$_4$(Au$_x$Ge$_{1-x}$)$_2$ ($x = 0.4$) appear to be in a 2+ oxidation state.

Keywords: Intermetallics; Silicides; Germanides; Flux synthesis

1. Introduction

Recently, liquid Al has been suggested as a solvent for the exploratory synthesis of new intermetallic phases [1–3]. Liquid Al facilitates the growth of large high-quality single crystals of complex intermetallic compounds, and this makes structural and physical characterization easier and more reliable. Synthetic explorations of the system RE/M/Al/Si(Ge) (RE = rare earth element, M = first row transition metal) produced a number of new multinary compounds, some with novel structures and interesting magnetic and electronic properties [4]. For example, investigations with Ni as the transition metal revealed the quaternary phases RENiAl$_4$(Ni$_x$Si$_{2-x}$), EuNiAl$_4$Si$_2$, RE_2NiAl$_4$Ge$_2$, and RENiAl$_4$Ge$_2$ [5]. Although these compounds crystallize in different structure types, all of them exhibit the stable building unit "NiAl$_4Tr_2$ (Tr = Si/Ge)".

The results obtained with the first and second row of transition metals stimulated interest in the third row. Gold is particularly active in Al flux and has resulted in a number of new phases such as the Th$_2$(Au$_x$Si$_{1-x}$)[AuAl$_2$]$_n$Si$_2$ homologous series [6], REAu$_4$Al$_8$Si [7], RE_2AuAl$_6$Si$_4$ [8] and REAu$_3$Al$_7$ [9]. These compounds feature hexagonal antifluorite-type slabs which can be regarded to be fragments of the bulk AuAl$_2$ structure. RE_2AuAl$_6$Si$_4$ is comprised of two different layers (a CaAl$_2$Si$_2$-type layer and a YNiAl$_4$Ge$_2$-type layer). The rich chemistry of the Si systems appears to be paralleled with Ge, but not in an identical fashion. Here we report results on the reactivity of Ge in aluminum flux and describe two families of quaternary compounds namely REAuAl$_4$Ge$_2$ (RE = Ce, Pr, Nd, Sm, Eu, Gd, Tb, Dy, Er, Tm and Yb) and REAuAl$_4$(Au$_x$Ge$_{1-x}$)$_2$ ($x = 0.4$) (RE = Ce and Eu).

*Corresponding author. Fax: +517 353 1793.
E-mail address: kanatzidis@chemistry.msu.edu (M.G. Kanatzidis).

0022-4596/$ - see front matter © 2005 Elsevier Inc. All rights reserved.
doi:10.1016/j.jssc.2005.07.029

2. Experimental section

2.1. Reagents

The following reagents were used as obtained: rare earth metals (RE = Ce, Pr, Nd, Sm, Eu, Gd, Tb, Dy, Er, Tm and Yb) (Cerac, 99.9%), Au (shavings from 1 ounce gold bullion, 99.99%), Al pellets (Cerac, 99.99%), Ge (Cerac, 99.999%).

2.2. Synthesis

***RE*AuAl$_4$Ge$_2$** (RE = Ce, Pr, Nd, Sm, Eu, Gd, Tb, Dy, Er, Tm and Yb): In a nitrogen-filled glove box, 1 mmol RE metal (0.14–0.18 g), 1 mmol Au (0.197 g), 10 mmol Al (0.270 g) and 5 mmol Ge (0.36 g) were combined in an alumina crucible. The crucible was then placed into a silica tube (13 mm in diameter), which was sealed under vacuum ($\sim 10^{-4}$ Torr). The samples were heated to 1000 °C in 12 h, maintained at this temperature for 30 h, then cooled to 850 °C in 24 h. They were annealed at 850 °C for 3 d, followed by cooling down to 500 °C in 72 h. Finally the temperature was brought down to 50 °C in 12 h.

***RE*AuAl$_4$(Au$_x$Ge$_{1-x}$)$_2$ ($x = 0.4$) (RE = Ce, Eu)**: In a nitrogen-filled glove box, 1 mmol RE metal (Ce 0.140 g, Eu 0.152 g), 1 mmol Au (0.197 g), 10 mmol Al (0.270 g) and 2 mmol Ge (0.1466 g) were combined in an alumina crucible. The crucible was then placed into a silica tube (13 mm in diameter), which was sealed under vacuum ($\sim 10^{-4}$ Torr). The samples were heated to 1000 °C in 12 h, maintained at this temperature for 5 h, then cooled to 850 °C in 24 h, finally slowly cooled down to 50 °C in 72 h.

The excess aluminum was removed by soaking the crucible in aqueous 5 M NaOH solution overnight. The solid product remaining after the isolation procedure was rinsed with water and acetone. The yields of each were ~80% for **1** REAuAl$_4$Ge$_2$ and ~90% for **2** REAuAl$_4$(Au$_x$Ge$_{1-x}$)$_2$ ($x = 0.4$) based on the initial amount of RE metal used in the reaction. Single crystals were selected for elemental analysis, X-ray diffraction and magnetic susceptibility measurements.

2.3. Elemental analysis

The crystals were fixed on the scanning electron microscope (SEM) sample plate using carbon tape. Chemical composition of the products was determined by energy dispersive spectroscopy (EDS) performed on JEOL JSM-35C SEM equipped with a NORAN EDS detector. Data were acquired by applying a 25 kV accelerating voltage with an accumulation time of 30 s. The atomic ratios in the compounds CeAuAl$_4$Ge$_2$ and EuAuAl$_4$(Au$_x$Ge$_{1-x}$)$_2$ were determined to be 1:1.25:4.87:2.1 (Ce:Au:Al:Ge) and 1:1.76:3.73:1.1 (Eu:Au:Al:Ge), which agreed well with the results derived from the single crystal X-ray data analysis.

2.4. X-ray crystallography

Single crystal X-ray diffraction data of **1** REAuAl$_4$Ge$_2$ were only collected for RE = Ce, Nd, Gd, Er and for **2** REAuAl$_4$(Au$_x$Ge$_{1-x}$)$_2$ ($x = 0.4$) (RE = Eu) at room temperature on a Bruker AXS SMART CCD X-ray diffractometer. A data collection (Mo $K\alpha$ radiation, $\lambda = 0.71073$ Å) was acquired covering either a full sphere or hemisphere of reciprocal space. Data processing was performed with the SAINT-PLUS software package [10]. An empirical absorption correction was applied to the data using the SADABS program [11]. The structures were solved straightforwardly using direct methods and refined with the SHELXTL package programs [12]. All atomic positions were refined with anisotropic thermal displacement parameters. The resulting stoichiometry agreed well with the elemental analysis from EDS. Tables 1 and 4 give crystallographic and refinement data for the structural analogs that were refined. Tables 2, 3 and 5 show the fractional atomic positions, equivalent thermal displacement parameters and selected bond distances.

The X-ray powder diffraction data were collected at room temperature on a CPS 120 INEL X-ray diffractometer (Cu $K\alpha$) equipped with position-sensitive detector. Experimental powder patterns were compared to the patterns calculated from the single crystal structure solution to determine the phase identity and purity.

2.5. Magnetic susceptibility measurements

Magnetic susceptibility measurements were conducted on the polycrystalline samples of **1** (CeAuAl$_4$Ge$_2$, EuAuAl$_4$Ge$_2$ and DyAuAl$_4$Ge$_2$) and **2** (CeAuAl$_4$(Au$_x$Ge$_{1-x}$)$_2$ and EuAuAl$_4$(Au$_x$Ge$_{1-x}$)$_2$ ($x = 0.4$)) using a Quantum Design MPMS SQUID magnetometer. EDS-analyzed crystals were ground into powder, which was sealed in kapton tape and placed into the magnetometer. The data were collected in the temperature range 3–300 K at 1000 G, while field-dependent magnetic measurements, conducted at 3 K, were carried out in fields up to $\pm 55{,}000$ G. A diamagnetic correction was applied to the data to account for core electron diamagnetism.

3. Results and discussion

3.1. Synthesis

The compounds REAuAl$_4$Ge$_2$ **1** were obtained with most rare earth elements and they tend to crystallize as plates or pyramidal crystals. Fig. 1 shows the SEM

Table 1
Crystal data and structure refinement details for REAuAl$_4$Ge$_2$ (RE = Ce, Nd, Gd, Er)

Empirical formula	CeAuAl$_4$Ge$_2$	NdAuAl$_4$Ge$_2$	GdAuAl$_4$Ge$_2$	ErAuAl$_4$Ge$_2$
Formula weight	590.19	594.31	581.11	671.29
Temperature	293(2) K	293(2) K	293(2) K	293(2) K
Wavelength	0.71073 Å	0.71073 Å	0.71073 Å	0.71073 Å
Space group	R-3m	R-3m	R-3m	R-3m
Lattice constants (Å)	a = 4.2384(7)	a = 4.2258(4)	a = 4.2123(6)	a = 4.2074(4)
	c = 31.613(7)	c = 31.359(5)	c = 30.994(6)	c = 30.717(5)
Volume	491.81(16)	484.97(10)	476.26(14)	470.91(9)
Z	4	4	4	4
Calculated density (g/cm^3)	7.971	8.140	8.104	9.468
Absorption coefficient (mm^{-1})	51.464	53.510	69.713	62.291
F(000)	1012	1020	948	1156
Crystal size (mm^3)	0.63 × 0.21 × 0.32	0.43 × 0.26 × 0.33	0.27 × 0.19 × 0.28	0.33 × 0.28 × 0.11
θ range (°)	1.93–27.63	11.22–37.15	11.25–37.25	11.27–37.00
Limiting indices	$-5 \leqslant h \leqslant 5$	$-7 \leqslant h \leqslant 7$	$-7 \leqslant h \leqslant 7$	$-7 \leqslant h \leqslant 6$
	$-5 \leqslant k \leqslant 5$	$-7 \leqslant k \leqslant 7$	$-7 \leqslant k \leqslant 7$	$-7 \leqslant k \leqslant 7$
	$-40 \leqslant l \leqslant 39$	$-52 \leqslant l \leqslant 52$	$-49 \leqslant l \leqslant 48$	$-51 \leqslant l \leqslant 51$
Reflections collected	1650	2487	2472	2448
Unique reflections	186	347	332	338
R_{int}	0.0454	0.0628	0.0635	0.0793
Completeness to θ	100.0%	93.3%	91.0%	94.4%
Refinement method	Full-matrix least-squares on F^2	Full-matrix least-squares on F^2	Full-matrix least-squares on F^2	Full-matrix least-squares on F^2
Variables	15	15	15	15
Goodness-of-fit on F^2	1.111	1.128	1.386	1.108
Final R indices [$I > 2\sigma(I)$][a]	R_1 = 0.0216,	R_1 = 0.0235,	R_1 = 0.0292,	R_1 = 0.0283,
	wR_2 = 0.0561	wR_2 = 0.0634	wR_2 = 0.0732	wR_2 = 0.0772
R indices (all data)	R_1 = 0.0216,	R_1 = 0.0235,	R_1 = 0.0298,	R_1 = 0.0297,
	wR_2 = 0.0561	wR_2 = 0.0634	wR_2 = 0.0741	wR_2 = 0.0780
Extinction coefficient	0.0120(7)	0.0111(7)	0.0107(8)	0.0134(10)
Highest residual peak (e Å^{-3})	1.589 and −2.358	2.920 and −4.494	5.918 and −3.765	2.732 and −4.754

$R_1 = \sum(|F_o| - |F_c|) \sum |F_o|$; w$R_2 = [\sum[w(F_o^2 - F_c^2]/[\sum(w|F_o|^2)^2]^{1/2}$.

Table 2
Atomic coordinates and equivalent isotropic displacement parameters (Å$^2 \times 10^3$) for CeAuAl$_4$Ge$_2$

Atom	Wyk. Symbol	x	y	z	$U_{(eq)}$[a]
Ce	3b	−0.6667	0.6667	0.1667	8(1)
Au	3a	0.0000	0.0000	0.0000	7(1)
Ge	6c	−0.3333	0.3333	0.1081(1)	8(1)
Al(1)	6c	−0.3333	0.3333	0.0245(1)	7(1)
Al(2)	6c	0.0000	0.0000	0.0820(1)	9(1)

[a] $U_{(eq)}$ is defined as one-third of the trace of the orthogonalized U_{ij} tensor.

Table 3
Selected bond lengths (Å)

	CeAuAl$_4$Ge$_2$	NdAuAl$_4$Ge$_2$	GdAuAl$_4$Ge$_2$	ErAuAl$_4$Ge$_2$
Ce–Ge	3.0692(7)	3.0341(4)	2.9901(6)	2.9516(5)
Au–Al(1)	2.5668(9)	2.5629(6)	2.5575(8)	2.5568(8)
Au–Al(2)	2.591(3)	2.5820(19)	2.578(3)	2.585(3)
Ge-Al(1)	2.5824(10)	2.638(2)	2.635(2)	2.645(3)
Ge–Al(2)	2.641(3)	2.5806(7)	2.5757(9)	2.5761(9)
Al(1)–Al(1)	2.897(3)	2.901(2)	2.902(3)	2.906(3)

images of typical single crystals of CeAuAl$_4$Ge$_2$ and EuAuAl$_4$(Au$_x$Ge$_{1-x}$)$_2$. The yields of the reactions were generally >80% based on the rare earth elements used. Side products were mainly recrystallized Ge and Au. Reactions with longer annealing times at 1000 °C did not improve the yields. Use of Yb as the RE metal produced the ternary compound YbAl$_2$Ge$_2$ instead of the target phase. Only when the amount of Yb was increased (from elemental ratio 1:1:10:5 to 3:1:10:5 for Yb:Au:Al:Ge), could YbAuAl$_4$Ge$_2$ be obtained as the main phase.

For Ce and Eu, when a much shorter heating profile was used, the phase REAuAl$_4$(Au$_x$Ge$_{1-x}$)$_2$ (x = 0.4) **2** was found to be the major product. When Sm was used under the same heating profile, only phase **1,** i.e. SmAuAl$_4$Ge$_2$, could be obtained. All compounds of **1** and **2** are stable in water and aqueous bases but dissolve in dilute acids.

3.2. Crystal structure of *1*

The REAuAl$_4$Ge$_2$ **1** crystallizes in a rhombohedral structure with space group R-3m. These compounds are

Table 4
Selected crystal data and structure refinement for $EuAuAl_4(Au_{1-x}Ge_x)_2$

Empirical formula	$EuAuAl_4(Au_{1-x}Ge_x)_2$
Formula weight	726.40
Temperature	293(2) K
Wavelength	0.71073 Å
Space group	*P*4/*mmm*
Unit cell dimensions	$a = 4.3134(8)$ Å
	$b = 4.3134(8)$ Å
	$c = 8.371(3)$ Å
Volume	155.75(7) Å^3
Z	1
Density (calculated)	7.745 Mg/m^3
Crystal Size (mm^3)	$0.046 \times 0.064 \times 0.052$
Independent reflections	146 [R(int) = 0.0533]
Completeness to $\theta = 28.25°$	96.7%
Refinement method	Full-matrix least-squares on F^2
Goodness-of-fit on F^2	1.151
Final R indices [$I > 2\sigma(I)$]	$R_1 = 0.0276$, w$R_2 = 0.0634$
R indices (all data)	$R_1 = 0.0289$, w$R_2 = 0.0642$
Largest diff. peak and hole	2.923 and −4.569 e Å^{-3}

Table 5
Atomic coordinates ($\times 10^4$) and equivalent isotropic displacement parameters (Å$^2 \times 10^3$) for $EuAuAl_4(Au_{1-x}Ge_x)_2$

	Wyk.Symbol	*X*	*Y*	*Z*	$U_{(eq)}$	Occu.
Au(1)	1*a*	0.0000	0.0000	0.0000	10(1)	1
Au(2)	2*h*	−0.5000	−0.5000	0.3462(1)	11(1)	0.411(4)
Ge	2*h*	−0.5000	−0.5000	0.3462(1)	11(1)	0.590(4)
Eu	1*b*	0.0000	0.0000	0.5000	13(1)	1
Al	4*i*	0.0000	−0.5000	0.1739(4)	12(1)	1

$U_{(eq)}$ is defined as one-third of the trace of the orthogonalized U_{ij} tensor.

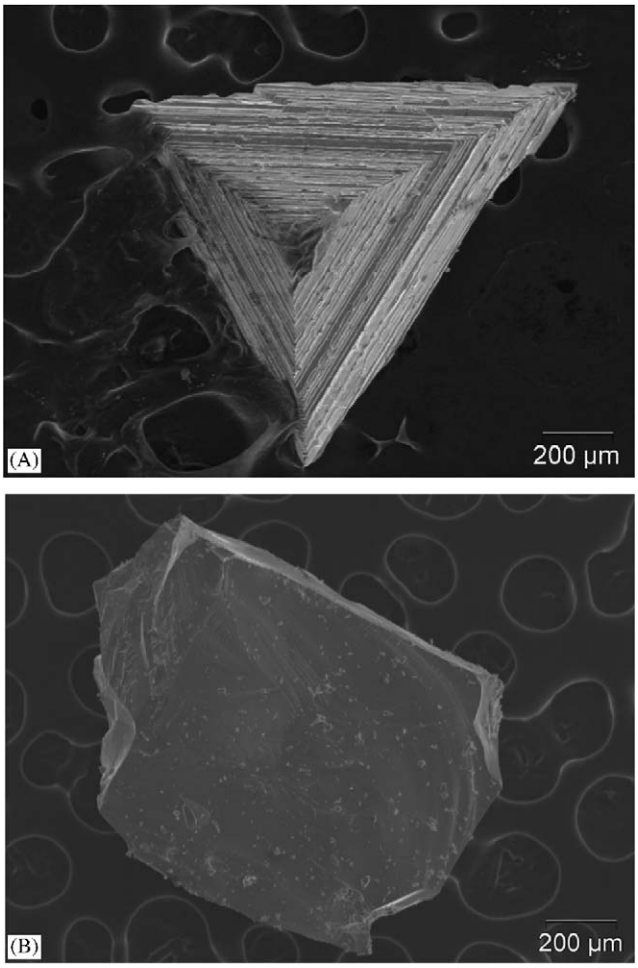

Fig. 1. SEM images of typical crystals of (A) $CeAuAl_4Ge_2$ and (B) $EuAuAl_4(Au_xGe_{1-x})_2$.

isostructural to $YNiAl_4Ge_2$ [13], which suggests that this structure type is robust and can accommodate a wide variety of non-isoelectronic transition metals. The difference between Ni and Au analogs is that $RENiAl_4Ge_2$ forms readily only with late *RE* metals, whereas almost all *RE* metals can form the Au analogs. That the $RENiAl_4Ge_2$ compounds form only with late *RE* metals could be due to the smaller size of $NiAl_4Ge_2$ slab (compared to $AuAl_4Ge_2$) which permits only the small *RE* ions to pack in the available space [4]. When the Ni atoms are replaced by the larger Au atoms in this structure, a cell parameter expansion is observed as expected, with the *a*-axis being much more expanded than the *c*-axis. This allows the larger rare earth elements to fit into the interlayer space. The unit cell parameters for Ce, Nd, Gd and Er analogs (Table 1), exhibit the sequential contraction as expected.

The structure of $CeAuAl_4Ge_2$ can be described as alternating layers of Ce atoms and $AuAl_4Ge_2$ slabs, Fig. 2. The bonds to the Ce atoms have been omitted in order to emphasize different layers in the structure. The Ce atoms in the *ab*-plane are close-hexagonally packed and form regular equilateral triangles with Ce–Ce distance of 4.2384(7) Å, corresponding to the length of the unit cell, *a* (Fig. 3A). Each Ce atom is 12-coordinated to GeAl(2) layers on both sides, see Fig. 3B.

The $[AuAl_4Ge_2]$ slab consists of distorted Al_8 cubes, with the lengths of the cube sides being 2.897(3) and 3.048 Å. Au atoms (as shown in Fig. 3C), held in the center of the cube, are surrounded by six Al(1) and two Al(2) atoms above and below to achieve square prismatic eight-coordinate environment. The Au–Al bond distances are 2.5668(9) and 2.591(3) Å, respectively, comparable to those in $AuAl_2$ (2.597 Å). These cubes are connected to each other via face sharing along the *ab*-plane.

The Ge atoms form puckered layers with Al(2) atoms which are in "chair" geometries when viewed down the *c* direction. Each Ge atom is surrounded by three Al(2) atoms and one Al(1) atom forming an umbrella-like geometry (shown in Fig. 3D). Similar coordination environment for Ge atoms is found in $AEAl_2Ge_2$

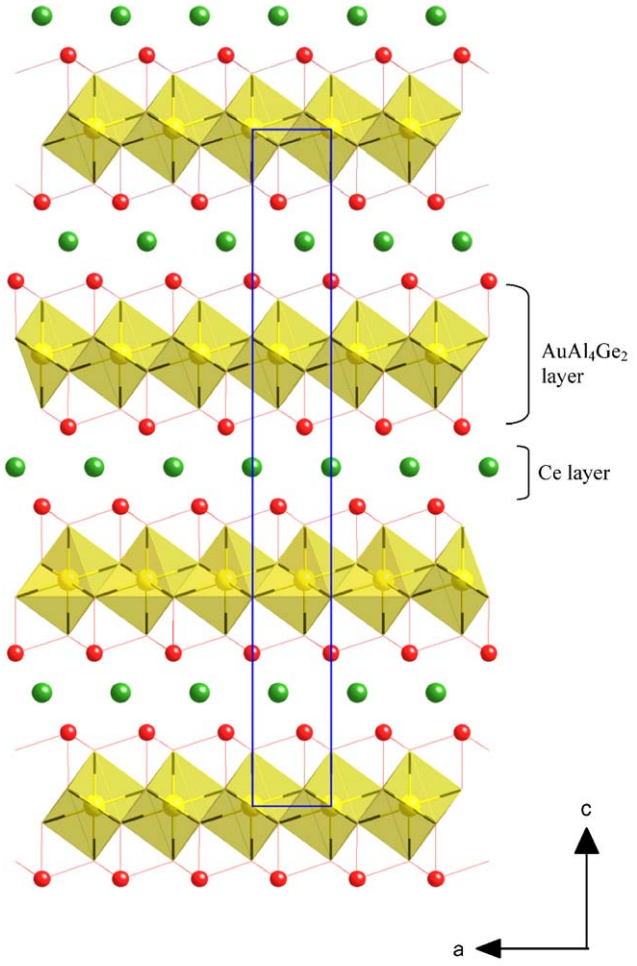

Fig. 2. Structure of $CeAuAl_4Ge_2$ viewed down the [010] direction. The $AuAl_4Ge_2$ layer is shown in polyhedral representation.

(AE = Ca, Sr) and $REAl_2Ge_2$ in which Ge atom is bonded to three Al atoms and one AE or RE atom [14].

3.3. Crystal structure of **2**

The compound **2** $EuAuAl_4(Au_xGe_{1-x})_2$ ($x = 0.4$) crystallizes in space group $P4/mmm$ with the KCu_4S_3 structure type. The same structure forms with other transition metals including Ni, Cu and Pd when Ge is replaced by Si [5]. As shown in Fig. 4A, the $AuAl_4(Au_xGe_{1-x})_2$ layers stack along the c-axis, and the Eu atoms reside in cages formed by eight Ge/Au atoms and four Al atoms, similar to those of the Ba atoms in the $BaAl_4$ structure type [15].

The $AuAl_4(Au_xGe_{1-x})_2$ layer contains a stable unit which occurs frequently in many intermetallic compounds, such as $LaGa_6Ni_{1-x}$ [16], $Tb_2NiAl_4Ge_2$ [4c], and Sm_2NiGa_{12} [17]. This layer can be described as follows: Au atoms are arranged in a square network with each Au atom sitting inside a distorted Al_8 cube. These cubes share edges with the Al–Al bond distance of 2.912(6) Å to form an infinite slab. The slab is then completed by capping Ge atoms on both sites. Analysis of the X-ray data shows that the capping atomic sites are in fact occupied by a mixture of Au and Ge atoms with a ratio of 2:3 [18]. The resulting $AuAl_4(Au_xGe_{1-x})_2$ layers stack and link to each other via Ge–Ge bonding between capping Ge atoms along the c direction. The distance between Au/Ge atoms across neighboring $AuAl_4(Au_xGe_{1-x})_2$ layers is 2.575(2) Å. As shown in Fig. 4B, the Eu atoms are arranged in a flat square-net, with an Eu–Eu distance of 4.3134(8) Å, which is equal to the a-cell parameter.

The coordination geometry of the Au atom is shown in Fig. 4C. The fully occupied Au position, which is bonded to eight Al atoms, exhibits a nearly cubic environment between two Al planar layers. The mixed Au/Ge site resides in a distorted tetragonal antiprism composed of Eu square plane and Al square plane (Fig. 4D). The mixed occupancy observed between Au and Ge is surprising given the very different nature of these two elements. It is however not unprecedented as similar phenomena are well known for example between Si and Ni [1]. One possible explanation is the similar electronegativities of the elements comprising the pair.

3.4. Magnetic properties

Magnetic susceptibility measurements were performed on polycrystalline samples produced by grinding selected single crystals.

3.5. Magnetism of **1**: ($CeAuAl_4Ge_2$, $EuAuAl_4Ge_2$, $DyAuAl_4Ge_2$)

The magnetic susceptibility as a function of temperature for $CeAuAl_4Ge_2$ is plotted in Fig. 5A. Up to 300 K, $CeAuAl_4Ge_2$ does not obey Curie–Weiss Law at any temperature range which indicates possible mixed Ce^{3+}/Ce^{4+} valence in this compound. The mixed or intermediate valence behavior, which is generally induced by the hybridization between 4f electrons and conduction electrons, has also been seen in other Ce-containing compounds such as $CeNiAl_4(Si_{2-x}Ni_x)$ and $Ce_2NiAl_{6-x}Ge_{4-y}$ [5]. We have calculated the magnetic moment of this compound from its susceptibility value χ_m measured at $T = 280$ K according to the equation $\mu_{exp} = 2.83(T\chi_m/6)^{1/2}(4\pi \times 10^{-6})$ BM. The resulting value $\mu_{exp} = 0.78$ BM is between the theoretical value of $\mu_{eff} = 0$ BM for Ce^{4+} and $\mu_{eff} = 2.54$ BM for Ce^{3+}. However, the temperature-dependent magnetic behavior of $CeAuAl_4Ge_2$ is different from well-known mixed valence systems such as $CeRu_3Si_2$ [19], the weakly mixed valence system $CeSn_3$ [20] and the strongly mixed valence system $CeRu_2$ [21]. In these typical mixed valence compounds, χ_m is almost constant at low

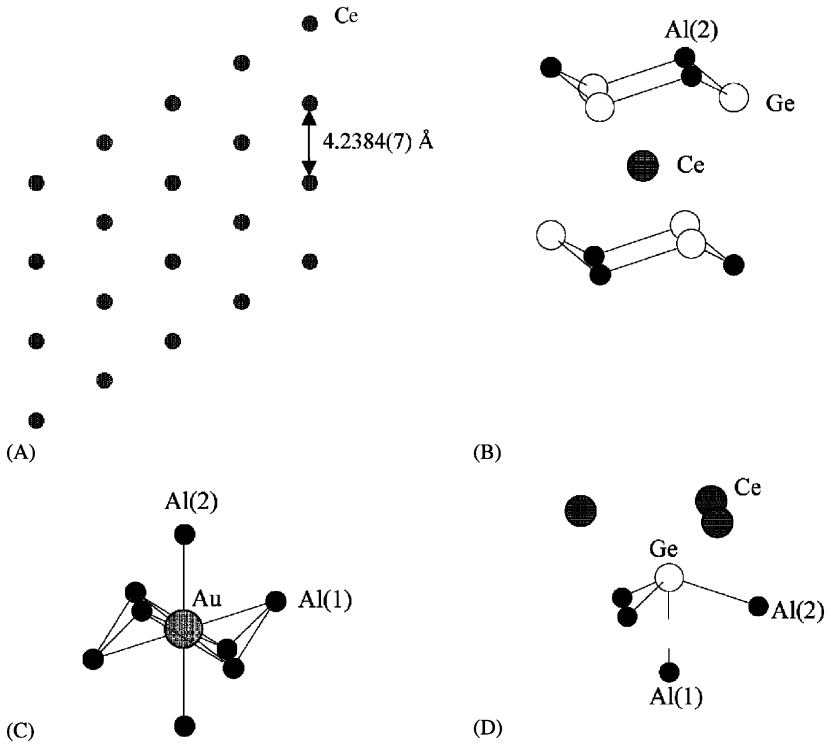

Fig. 3. Structure of $CeAuAl_4Ge_2$. (A) Trigonal pattern of Ce atoms in *ab*-plane; (B,C,D) coordination environments of Ce, Au and Ge atoms.

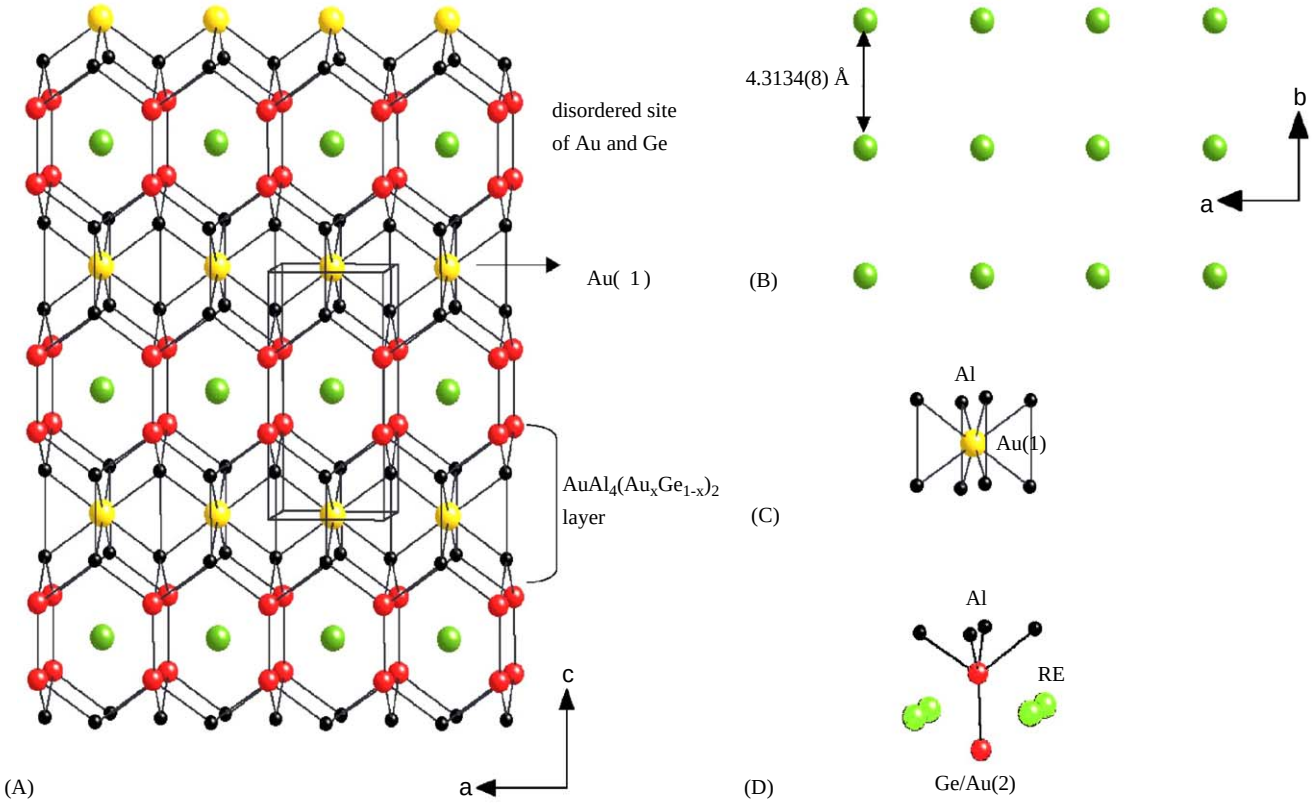

Fig. 4. Structure of $EuAuAl_4(Au_xGe_{1-x})_2$. (A) The $EuAuAl_4(Au_xGe_{1-x})_2$ structure viewed down the [010] direction; (B) the square net formed by Eu atoms in the *ab*-plane; (C) and (D) local coordination environments of Au(1) and Ge atoms.

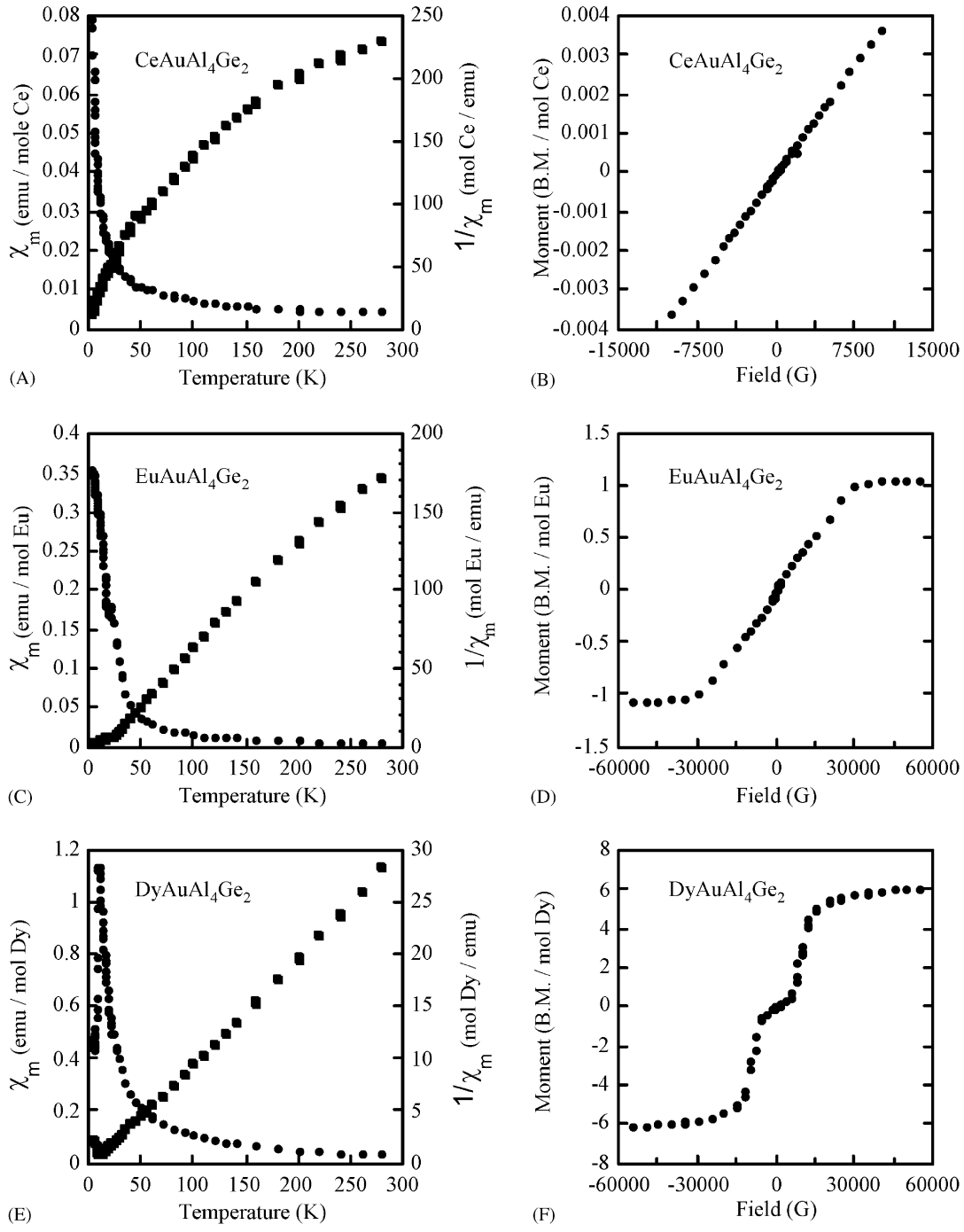

Fig. 5. (A) Temperature-dependent magnetic susceptibility of $CeAuAl_4Ge_2$; (B) field-dependent magnetization at 3 K for $CeAuAl_4Ge_2$; (C) temperature-dependent magnetic susceptibility of $EuAuAl_4Ge_2$; (D) field-dependent magnetization at 3 K for $EuAuAl_4Ge_2$; (E) temperature-dependent magnetic susceptibility of $DyAuAl_4Ge_2$; (F) field-dependent magnetization at 3 K for $DyAuAl_4Ge_2$.

temperatures, it then increases with increasing temperature and tends to obey the Curie–Weiss Law at high temperatures. The reason that $CeAuAl_4Ge_2$ shows different magnetic behavior from typical mixed valence compounds might be that it is a very weakly mixed-valence system that has a much lower fluctuation temperature. Fig. 5B shows the magnetization of $CeAuAl_4Ge_2$ as a function of field. The magnetization is increasing linearly up to 10,000 G without saturation.

The magnetic susceptibility of $EuAuAl_4Ge_2$ obeys the Curie–Weiss Law above 50 K, Fig. 5C. The μ_{eff} value, obtained from the data, is 3.34 BM, while that of free-ion for Eu^{3+} is 3.40 BM. Therefore, we can regard the oxidation state of Eu ion as 3+, while Au is diamagnetic

as it was seen in $DyAuAl_4Ge_2$. Because of the slightly enhanced stability of half-filled $4f$ shells of Eu^{2+}, most europium compounds show divalent europium or mixed valence of Eu^{2+}/Eu^{3+}. To further determine the oxidation state of Eu atoms, ^{151}Eu Mössbauer Spectroscopy might be needed. The field-dependent data (Fig. 5D) shows a gradual increase of the magnetization until saturation which occurs at about 30,000 G; however, magnetization per Eu ion at this point is only 30% of the maximum value calculated according to the formula $\mu_{Eu(calc)} = gJ$ BM (for a free atom the g factor is defined by the Landé equation, the total angular momentum J is the sum of the orbital L and spin S angular momenta).

The molar magnetic susceptibility data of $DyAuAl_4Ge_2$ vs temperature is plotted in Fig. 5E. This material exhibits an antiferromagnetic transition at low temperature around 11 K and conforms to the Curie–Weiss Law behavior above the transition temperature. The calculated μ_{eff} (9.17 BM) is somewhat lower than the theoretical value for Dy^{3+} (10.63 BM), as is frequently observed, and the difference might be ascribed to the crystal-field effects [22]. The measured magnetic moment is entirely attributed to Dy atoms with the Au atoms being diamagnetic.

$DyAuAl_4Ge_2$ exhibits field-induced metamagnetic behavior at 3 K, as shown in Fig. 5F. A gradual increase in magnetization is observed until the field reaches 5000 G where a dramatic increase occurs, indicating spin reorientation. Then the magnetization begins to saturate and does not change much up to 55,000 G. However, the moment per Dy^{3+} ion at this point is only 60% of its maximum value (10.60 BM) which is calculated from $\mu_{Dy(calc)} = gJ$ BM. The sharp jump occurring at 5000 G suggests a possible transition to a more ferromagnetically ordered state, which can also be supported by the positive sign of the Weiss constant θ. Similar spin complexity has been observed in other intermetallic compounds including $Dy_2AuAl_6Si_4$ [8] and β-$DyNiGe_2$ [23]. It has been suggested that a trigonal arrangement of rare earth ions on a plane could create frustration in antiferromagnetic coupling [24]. A field higher than 55,000 G may be required to achieve complete saturation of the magnetization.

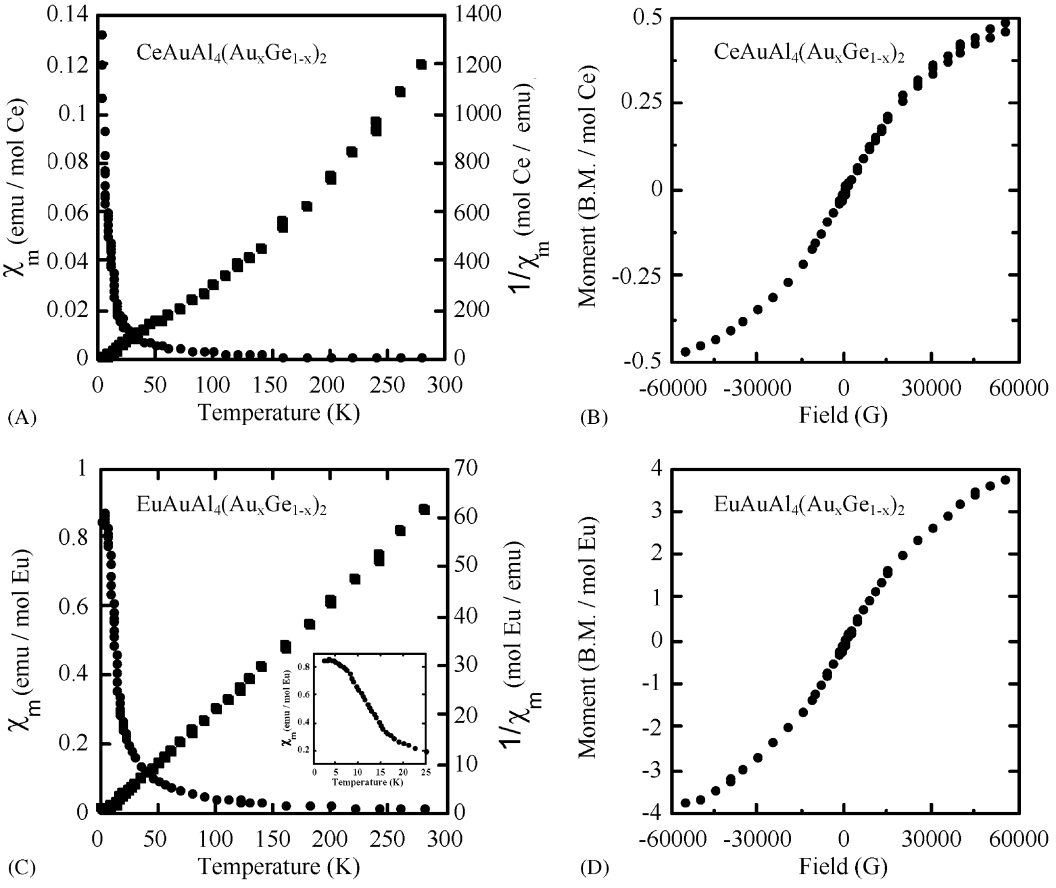

Fig. 6. (A) Temperature-dependent magnetic susceptibility of $CeAuAl_4(Au_xGe_{1-x})_2$; (B) field-dependent magnetization at 3 K for $CeAuAl_4(Au_xGe_{1-x})_2$; (C) temperature-dependent magnetic susceptibility of $EuAuAl_4(Au_xGe_{1-x})_2$; (D) field-dependent magnetization at 3 K for $EuAuAl_4(Au_xGe_{1-x})_2$.

3.6. Magnetism of 2: ($CeAuAl_4(Au_xGe_{1-x})_2$, $EuAuAl_4(Au_xGe_{1-x})_2$)

Fig. 6A gives the thermal dependence of the magnetic susceptibility χ_m measured for $CeAuAl_4(Au_xGe_{1-x})_2$. The μ_{eff} values, calculated by fitting to the Curie–Weiss Law in the temperature range of 50–140 K and 160–300 K, are 1.54 and 1.18 BM, respectively, which are between the theoretical ones of $\mu_{eff} = 0$ BM for Ce^{4+} and $\mu_{eff} = 2.54$ BM for Ce^{3+}. The change in the slope of inverse susceptibility plot may be due to changes in the Ce valence state over the whole temperature range. This behavior is different from those compounds with intermediate valence of Ce atoms, which also obeys the Curie–Weiss Law at high temperature while Ce atoms are in 3+ oxidation state [25]. The Au atoms are likely diamagnetic as in the other Al-grown intermetallic compounds described above.

For $EuAuAl_4(Au_xGe_{1-x})_2$, the temperature-dependent magnetic susceptibility data at 1000 G show an antiferromagnetic transition at about 4 K, as shown in the inset of Fig. 6C. The magnetization increases gradually with increasing applied field. No magnetization saturation is observed up to 55,000 G (Fig. 6D). When the high-temperature (above 20 K) data are fit to the Curie–Weiss Law, a μ_{eff} of 6.03 BM is obtained. The calculated effective magnetic moment for Eu^{2+} $4f^7$ ions is predicted to be equal to the value of Gd^{3+} ions, which is 7.94 BM. Thus, we suggest that Eu ions in this compound $EuAuAl_4(Au_xGe_{1-x})_2$ are in a divalent $4f^7$ ground state and the difference might due to the crystal-field effects. This observation is consistent with the statement that Eu is often found to be divalent in noble-metal compounds with a broad *s* band. Examples include $EuAg_5$ [26], $EuAu_5$ [27], EuAuMg [28], $Eu(Pd_{1-x}Au_x)_2Si_2$ [29] and $EuAu_4Al_8Si$ [7].

4. Concluding remarks

A rich intermetallic chemistry is possible in liquid Al. As a result of exploratory synthesis in the system *RE*/Au/Al/Ge using Al as the flux, two families of quaternary intermetallic compounds $REAuAl_4Ge_2$ (*RE* = Ce, Nd, Sm, Eu, Gd, Dy, Er and Yb) and $REAuAl_4(Au_xGe_{1-x})_2$ ($x = 0.4$) (*RE* = Ce and Eu) have been obtained.

The magnetic moments are localized on the *RE* atoms and Au atoms are in non-magnetic state. Antiferromagnetic ordering transitions are observed in $DyAuAl_4Ge_2$ and $EuAuAl_4(Au_xGe_{1-x})_2$ with Néel temperature of 11 and 4 K, and $DyAuAl_4Ge_2$ exhibits metamagnetic behavior at 3 K. The Ce analogs may exhibit valence fluctuations in the temperature range measured.

5. Supporting information available

Tables of crystallographic details, atomic coordinates, isotropic and anisotropic thermal displacement parameters, bond distances and angles for $CeAuAl_4Ge_2$, $NdAuAl_4Ge_2$, $GdAuAl_4Ge_2$, $ErAuAl_4Ge_2$ and $EuAuAl_4(Au_xGe_{1-x})_2$ are available. This information can be obtained from the Fachinformationszentrum Karlsruhe, 76344 Eggenstein-Leopoldshafen, Germany (Fax: (49) 7247-808-666; E-mail: crysdata@fiz-karlsruhe.de); the depository numbers for $CeAuAl_4Ge_2$, $NdAuAl_4Ge_2$, $GdAuAl_4Ge_2$, $ErAuAl_4Ge_2$ and $EuAuAl_4(Au_xGe_{1-x})_2$ are 415287-415291.

Acknowledgments

This work made use of the SEM/EDS facilities of the Center for Electron Optics at Michigan State University. Financial support from the Department of Energy (Grant # DE-FG02-99ER45793) is gratefully acknowledged. We thank Dr. S.E. Latturner for useful discussions during the preparation of the manuscript.

References

[1] (a) X.Z. Chen, S. Sportouch, B. Sieve, P. Brazis, C.R. Kannewurf, J.A. Cowen, R. Patschke, M.G. Kanatzidis, Chem. Mater. 10 (1998) 3202;
(b) B. Sieve, X.Z. Chen, J. Cowen, P. Larson, S.D. Mahanti, M.G. Kanatzidis, Chem. Mater. 11 (1999) 2451;
(c) X. Wu, D. Bilc, S.D. Mahanti, M.G. Kanatzidis, Chem. Commun. 9 (2004) 1506.
[2] (a) V.M.T. Thiede, B. Fehrmann, W. Jeitschko, Z. Anorg. Allg. Chem. 625 (1999) 1417;
(b) B. Fehrmann, W. Jeitschko, J. Alloy Compd. 298 (2000) 153.
[3] M.G. Kanatzidis, R. Pöttgen, W. Jeitschko, Angew. Chem. Int. Ed. (2005), in press.
[4] (a) B. Sieve, S. Sportouch, X.Z. Chen, J.A. Cowen, P. Brazis, C.R. Kannewurf, V. Papaefthymiou, M.G. Kanatzidis, Chem. Mater. 13 (2001) 273;
(b) B. Sieve, X.Z. Chen, R. Henning, P. Brazis, C.R. Kannewurf, J.A. Cowen, A.J. Schultz, M.G. Kanatzidis, J. Am. Chem. Soc. 123 (2001) 7040;
(c) B. Sieve, P.N. Trikalitis, M.G. Kanatzidis, Z. Anorg. Allg. Chem. 628 (2002) 1568.
[5] B. Sieve, Ph.D. Dissertation, Michigan State University, 2002.
[6] S.E. Latturner, D. Bilc, S.D. Mahanti, M.G. Kanatzidis, Chem. Mater. 14 (2002) 1695.
[7] S.E. Latturner, M.G. Kanatzidis, Chem. Commun. 18 (2003) 2340.
[8] S.E. Latturner, M.G. Kanatzidis, Inorg. Chem. 42 (2003) 7959.
[9] S.E. Latturner, D. Bilc, J.R. Ireland, C.R. Kannewurf, S.D. Mahanti, M.G. Kanatzidis, J. Solid State Chem. 170 (2003) 48.
[10] Saint, version 4, Simens Analytical X-ray Instruments Inc., Madison, WI.
[11] G.M. Sheldrick, SADABS, University of Göttingen, Göttingen, Germany.
[12] G.M. Sheldrick, SHELXTL. Structure Determination Programs, Version 5.0, Siemens Analytical X-ray Instruments Inc., Madison, WI, 1995.

[13] B. Sieve, X. Chen, J. Cowen, P. Larson, S.D. Mahanti, M.G. Kanatzidis, Chem. Mater. 11 (1999) 2451.
[14] C. Kranenberg, D. Johrendt, A. Mewis, Solid State Sci. 4 (2002) 261.
[15] K.R. Andress, E. Alberti, Z. Metallkd. 27 (1935) 126.
[16] Yu.N. Grin, Ya.P. Yarmolyuk, I.V. Rozhdestvenskaya, E.I. Gladyshevskii, Kristallografiya 27 (1982) 693.
[17] X.Z. Chen, P. Small, S. Sportouch, M. Zhuravleva, P. Brazis, C.R. Kannewurf, M.G. Kanatzidis, Chem. Mater. 12 (2000) 2520.
[18] The Si analogues grown from Al flux such as $REAu_4Al_8Si$ also has the mixed occupied site of Au and Si with the ratio 1:1. Our assignment in the compound $EuAuAl_4(Au_xGe_{1-x})_2$ supports the assignment that the mixed occupied site in $REAu_4Al_8Si$ is in fact between Au and Si instead of Au and Al.
[19] Y. Kishimoto, Y. Kawasaki, T. Ohno, Phys. Lett. 317 (2003) 308.
[20] (a) J.M. Lawrence, P.S. Riseborough, R.D. Parks, Rep. Prog. Phys. 44 (1981) 1;
(b) J.M. Lawrence, P.S. Riseborough, R.D. Parks, in: L.M. Falicov, W. Hanke, M.B. Maple (Eds.), Valence Fluctuations in Solids, North-Holland, Amsterdam, 1981.
[21] A.V. Tsvyashchenko, L.N. Fomicheva, A.A. Sorokin, G.K. Ryasny, B.A. Komissarova, L.G. Shpinkova, K.V. Klementiev, A.V. Kuznetsov, A.P. Menushenkov, V.N. Trofimov, A.E. Primenko, R. Cortes, Phys. Rev. B 65 (2002) 174513.
[22] C. Kittel, Introduction to Solid State Physics, Seventh ed., Wiley, New York, 1996, p. 426.
[23] J.R. Salvador, J.R. Gour, D. Bilc, S.D. Mahanti, M.G. Kanatzidis, Inorg. Chem. 43 (2004) 1403.
[24] D. Gignoux, D. Schmitt, J. Alloy Compd. 326 (2001) 143.
[25] (a) B. Chevalier, J.L. Bobet, E. Gaudin, M. Pasturel, J. Etourneau, J. Solid State Chem. 168 (2002) 28;
(b) J. Tang, K.A. Gschneidner, Phys. Rev. B 52 (1995) 7328.
[26] E.V. Sampathkumaran, B. Perscheid, G. Kaindl, Solid State Commun. 51 (1984) 701.
[27] F.J. Van Steenwijk, W.J. Huiskamp, H.Th. Lefever, R.C. Thiel, K.H.J. Buschow, Physica B & C 86–88B (1997) 89.
[28] R. Pottgen, R. Hoffmann, J. Renger, U.C. Rodewald, M.H. Moller, Z. Anorg. Allg. Chem. 626 (2000) 2257.
[29] M.M. Abd-Elmeguid, Ch. Sauer, U. Koebler, W.Z. Zinn, Phys. B: Condens. Matter 60 (1985) 239.